

Model of Uptake of OH Radicals on Nonreactive Solids

R. G. Remorov* and M. W. Bardwell

Department of Chemistry, University of Waterloo, 200 University Avenue West, Ontario N2L 3G1, Canada

Received: April 4, 2005; In Final Form: August 24, 2005

A model of adsorption and recombination of OH radicals was developed for nonreactive solid surfaces of atmospheric interest. A parametrization of this heterogeneous mechanism was carried out to determine the role of the catalytic properties of these solid surfaces, taking into account the adsorption energy, defects, surface diffusion, and chemical reactions in the gas–solid interface. The uptake process was simulated for diffusion-controlled chemical reactions on the surface on the basis of Langmuir–Hinshelwood and Eley–Rideal mechanisms. Using an analytical approach and the Monte Carlo technique, we show the dependencies of the uptake probability of the heterogeneous reactions on the OH concentration and adsorption energy. The model is employed in the analysis of the empirically derived uptake coefficient for water ice, Al_2O_3 , NaCl, NH_4NO_3 , NH_4HSO_4 , and $(\text{NH}_4)_2\text{SO}_4$. We found the following values for the free energy of adsorption of OH radicals: $E_{\text{ice}} = 7.3\text{--}7.6$ kcal/mol, $E_{\text{Al}_2\text{O}_3} = 11\text{--}11.7$ kcal/mol, $E_{\text{NH}_4\text{NO}_3} = 10.2$ kcal/mol, $E_{\text{NaCl}} = 10.2$ kcal/mol, $E_{\text{NH}_4\text{HSO}_4} = 9.8$ kcal/mol, and $E_{(\text{NH}_4)_2\text{SO}_4} = 9.8$ kcal/mol. The atmospheric implications of the catalytic reactions of OH with adsorbed reactive molecules are discussed. The results of the modeling of the uptake process showed that the heterogeneous decay rate can exceed the corresponding gas-phase reaction rate under atmospheric conditions.

Introduction

Gas–solid interfacial phenomena play a key role in multiphase processes in atmospheric chemistry, affecting cloud and aerosol properties and influencing the radiation balance of the earth. The study of the heterogeneous processes occurring on solid surfaces has been the objective of intensive work for the past decade. It is well-known that the chemical composition of aerosols is a function of the interface properties associated with the kinetics of the heterogeneous chemical transformation of trace species and their accommodation.¹

Studying uptake processes of OH radicals is of great importance in both environmental issues and heterogeneous catalysis. The interest in studying atmospheric reactions with OH radicals has been motivated by the role of OH and HO_2 radicals in the oxidative transformation of pollutants in the troposphere. The change in the HO_x concentration affects the balance of such ozone-active species as NO_x , ClO_x , and BrO_x . Moreover, HO_x radicals participate in the hydrogen cycle of tropospheric ozone destruction. OH radicals play a key role in the oxidation of the most volatile organic compounds (VOCs) in the atmosphere.²

Uptake processes of gas-phase species by solid surfaces can be described by a parameter such as the uptake coefficient, γ . The uptake coefficient is a dimensionless parameter that is defined as the probability of the removal of a gas-phase species through interaction with the condensed phase. Recent laboratory studies of OH uptake on a number of different solids demonstrated that the uptake coefficient varies in the range of $10^{-3}\text{--}10^{-2}$.^{3,4} Cooper and Abbatt were the first to study the interaction of OH radicals with water ice, NH_4HSO_4 , and $(\text{NH}_4)_2\text{SO}_4$ using a laminar coated-wall flow tube coupled to a resonance fluorescent detector. The measured value of the OH uptake coefficient ($\text{OH} < 10^{10}$ radicals/ cm^3) suggested a first-order decay rate of OH for nonporous polycrystalline solids.

Ivanov et al. studied the uptake of OH on the solid salts NaCl and NH_4NO_3 using a flow reactor with a rod that is variable in length. A negative temperature dependence was observed for solid NaCl and NH_4NO_3 in the temperature range of 245–340 K. The authors concluded that the heterogeneous decay of OH radicals is of minor importance in the troposphere as a result of the high reactivity of OH radicals in the gas phase.

Solid atmospheric salt aerosols do not have a considerable adsorption capacity. However, it is well-known that adsorption of ClONO_2 , N_2O_5 , NO_3 , and NO_2 onto NaCl aerosols followed by their subsequent reactions with NaCl particles results in the formation of Cl-containing compounds and, hence, an increase in Cl-containing compounds in the troposphere.^{5–8} Catalytic properties of salt aerosols in the OH radical initiated atmospheric oxidation of VOCs were extensively studied by Oh and Andino and by Sorensen et al.^{9–12} Although the conditions of these studies were very close to each other, they obtained contradicting results in a study of the influence of solid aerosols of $(\text{NH}_4)_2\text{SO}_4$ and NH_4NO_3 on the reaction of OH with VOCs, such as CH_3OH and $\text{C}_2\text{H}_5\text{OH}$.¹² In particular, Sorensen et al.¹² found that, according to the prediction based on an Eley–Rideal (ER) mechanism,⁸ heterogeneous reactions of OH radicals with organics cannot cause the considerable drop in the concentration of the organic compounds in the presence of solid aerosols.

Langmuir–Hinshelwood (LH) and ER reaction schemes are widely used for the description of the elementary heterogeneous reactions in the gas–solid and gas–liquid interface.^{13–15} Ammann et al. reported an analytical expression for the uptake in the case of Langmuir type equilibrium between gas phase and adsorbed species at the gas–liquid interface.¹⁵ They assumed a bimolecular mechanism of the reaction in the suggestion of the pseudo-first-order kinetics. For the case of the heterogeneous reaction of OH with solids, the uptake process may include the recombination of radicals. Therefore, the

* Corresponding author. E-mail address: rremorov@sciborg.uwaterloo.ca.

TABLE 1: Measured Uptake Coefficients for Different Solid Substrates

substrate	uptake coefficient	T, K	ref
water ice	0.03 ± 0.02	205–230	3
(NH ₄) ₂ SO ₄	0.0085	296	3
NH ₄ HSO ₄	0.002	296	3
NaCl	4.1 × 10 ⁻³	300	4
	(1.2 ± 0.7) × 10 ⁻⁵ exp[(1750 ± 200)/T]	245–340	4
NH ₄ NO ₃	3.9 × 10 ⁻³	300	4
	(1.4 ± 0.5) × 10 ⁻⁴ exp[(1000 ± 100)/T]	245–340	4
Al ₂ O ₃	0.04	295	36
	0.11		40

application of LH and ER mechanisms requires an additional analysis for the real atmospheric conditions.

The role of catalytic processes on the loss of the atmospheric pollutants in the presence of OH radicals is not clear. In particular, there is no theoretical model which can explain the behavior of the OH uptake process in the presence of the reagent in the gas phase. Thus, it is highly desirable to develop a quantitative model to describe such processes.

The aim of this work was to study the catalytic role of surfaces of atmospheric salt aerosols and their impact on the uptake kinetics in the presence of organic or inorganic compounds. The main goal of this work is to use an analytical approach in the description of the gas–solid interfacial reactions so that the basic features of the elementary heterogeneous steps can be determined. The mechanism of the reaction between adsorbed radicals was considered by Remorov et al.¹⁶ for the HO₂ uptake on NaCl based on LH and ER reaction schemes. In the work reported herein, an advanced model is presented for diffusion-controlled surface reactions on nonreactive solids.

Description of the Model for the Adsorption of OH

The measured uptake coefficients for different substrates are summarized in Table 1. Although the uptake coefficient exhibits time-dependent behavior, Table 1 represents stationary values of the uptake coefficients (exposure time exceeded 5–10 min).

Table 1 shows that the reactivity of OH radicals toward inert substrates, such as water ice and sulfate, does not differ from that for the more reactive ammonium bisulfate and sodium chloride. Note that the possible chemical reaction of OH radicals with NaCl can produce hypochlorous acid, HOCl, via the reaction



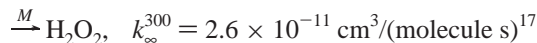
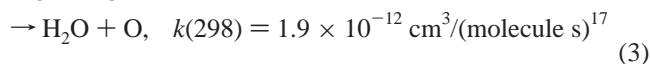
However, from the upper limit of the uptake coefficient (<4 × 10⁻³), it may be concluded that the uptake process is not limited by the reaction of OH radicals with the substrate. Another feature of the uptake on the nonreactive salts is that the uptake coefficient has a negative Arrhenius dependence, which could be explained by physical adsorption of radicals as a precursor to a reaction.¹³

Thus, one possible explanation of the similarity of the uptake coefficients among different solid substrates is that the uptake process is limited by diffusion-controlled recombination reactions on the surface. We consider the uptake process occurring on the surface through the reaction between OH radicals by the following scheme:

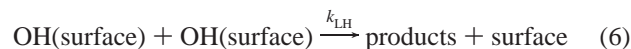
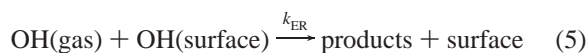


Reaction 2 is not elementary. This reaction includes the

recombination of radicals on the surface analogously to the homogeneous reaction in the gas phase.



Adsorption of OH radicals can occur on specific sites. Schemes of heterogeneous reactions may include both ER and LH mechanisms.¹³ For the ER scheme, the adsorbed species can react with gas-phase radicals in a direct elementary reaction. The reaction between two adsorbed species is usually referred to as the LH mechanism.¹³ For LH kinetics, we assume that two adsorbed radicals can diffusively migrate on the surface and react on the active sites:



where k_1 is the adsorption rate constant (in cm/s), k_{-1} is the desorption rate constant (in s⁻¹), and k_{ER} (in cm/s) and k_{LH} (in cm²/s) are the ER and LH reaction rate constants, respectively.

The adsorption rate constant, k_1 , is defined from molecular kinetic theory as the following: $k_1 = \alpha c_{\text{OH}}/4$, where α is the accommodation coefficient, which was further set equal to unity, and c_{OH} is the thermal speed of the radicals.

The desorption rate constant, k_{-1} , can be expressed in the form^{13,14}

$$k_{-1} = \frac{kT}{h} \exp\left(-\frac{E_{\text{OH}}}{RT}\right) \quad (7)$$

where E_{OH} is the free energy of adsorption and k and h are the Boltzmann and Planck constants, respectively. k_{ER} is defined according to scheme 5:

$$k_{\text{ER}} = \beta_{\text{ER}} \frac{c_{\text{OH}}}{4} \quad (8)$$

where β_{ER} is the probability of the reaction according to the scheme 5.

Reactions 4–6 result either in the liberation of the surface site or in the adsorption of the reaction product on the surface site. In our simulations, we postulated that the products of reactions 5 and 6 do not inhibit radical uptake. This is a reasonable assumption for the low extent of coverage that corresponds to a realistic atmospheric environment.

For the description of the uptake of OH radicals we used the concept of localized adsorption for which the molecules or radicals are considered to be adsorbed on discrete sites where they reside in the position of minimum potential energy.¹⁸ To describe the uptake of molecules by the solid surface we used the Langmuir approach, which assumes local adsorption equilibrium. Let us consider the adsorbed molecules as an average monolayer that is in equilibrium between the gas phase and the solid phase. The surface coverage, θ_{OH} , is determined by the ratio of the surface concentration to the maximum surface density, Z_{OH} (in cm⁻²), for given surface radicals, $\theta_{\text{OH}} = n_{\text{sOH}}/Z_{\text{OH}}$, where n_{sOH} (in cm⁻²) is the surface concentration of radicals. For simplicity, we postulated that the maximum surface

densities for radicals and gas-phase species are equal and correspond to the surface density of the Na^+Cl^- ionic pairs, $Z_{\text{OH}} = 6.4 \times 10^{14} \text{ cm}^{-2}$.¹³ The ER reaction rate (5) is determined by the expression

$$J_{\text{ER}} = k_{\text{ER}} n_{\text{OH}} \theta_{\text{OH}} Z_{\text{OH}} \quad (9)$$

where n_{OH} (in cm^{-3}) is the gas-phase concentration of OH radicals.

We suggested in our modeling that the probability of the recombination (5) is close to one. It means that

$$k_{\text{ER}} = \frac{c_{\text{OH}}}{4} \quad (10)$$

This suggestion is reasonable because the gas-phase consumption of the OH radicals for the reaction of the recombination is fast under atmospheric conditions.

The coverage of adsorbed radicals is a function of the basic physicochemical parameters such as the adsorption and desorption rates, the chemical reaction rate constant, the surface concentration of radicals (coverage), and the defect concentration. In our investigation we neglect mutual interactions between radicals. This is reasonable for typical laboratory experiments and atmospheric conditions with low coverage of radicals on the surface.

A theoretical description of the chemical reaction in two dimensions was derived in the work of Freeman and Doll.¹⁹ For a chemical reaction occurring on the solid surface, the rate constant k_{LH} is defined from the continuum model:

$$\frac{1}{k_{\text{LH}}} = \frac{1}{k_{\text{LH}}^{\text{d}}} + \frac{1}{k_{\text{LH}}^{\text{k}}} \quad (11)$$

where k_{LH}^{d} (in cm^2/s) is the diffusion-limited rate constant and k_{LH}^{k} (in cm^2/s) is the surface rate constant of the bimolecular reaction. A theoretical framework of diffusion-limited kinetics in two dimensions using a hopping approach, a continuum model, and the Monte Carlo (MC) technique were considered by a number of authors.^{19–21} Allen and Seebauer²⁰ studied the diffusion kinetics $\text{A} + \text{A} \rightarrow \text{A}_2$ in two dimensions. They found that continuum and hopping models yield a simple relation between the surface diffusion and the rate constant and the coverage:

$$k_{\text{LH}}^{\text{d}} = \frac{2\pi D_{\text{s}}}{\ln(\sqrt{1/\theta})} \quad (12)$$

where D_{s} (in cm^2/s) is the surface diffusion. Equation 12 demonstrates that the two-dimensional diffusion-controlled chemical reaction is a function of the coverage θ . The continuum model (eq 12) fails when the coverage θ exceeds 10^{-3} .²⁰ For short times or high coverage, an analytical expression of the diffusion-controlled reaction rate constant was derived:

$$k_{\text{LH}}^{\text{d}} = \frac{\pi D_{\text{s}}}{y} \quad (13)$$

where y is the two-dimensional packing fraction. For square lattice symmetry, $y = \pi/4$.²⁰

Several kinetic theories for chemical reactions in the condensed phase in two dimensions were developed^{19,22–25} on the basis of an analytical approach, quantum-chemical calculations, and MC techniques. There is no literature data of the surface-reactive rate constant k_{LH} for the reaction $\text{OH} + \text{OH}$. However,

the high limit of the surface-reactive rate constant k_{LH} may be estimated from the lattice-gas model.²⁵ According to the lattice-gas model, effective heterogeneous rate constants for the elementary processes between two adsorbed species may be estimated from the molecular-gas kinetic theory, taking into account the interaction of the adsorbed molecules with active sites. The upper limit of the reaction rate constant between adsorbed radicals in the layer of the thickness δ may be estimated from the corresponding gas-phase reaction as $k_{\delta} \approx k_{\text{g}}/\delta$.

The upper limit of the heterogeneous rate constant is determined by k_{δ} because the surface influence on the chemical kinetics is ignored in this case. The estimation of k_{δ} for the recombination rate constant in the layer of adsorbed radicals ($\sim 3 \text{ \AA}$)²⁶ gives $k_{\delta} \approx 3 \times 10^{-4} \text{ cm}^2/\text{s}$. Note that the high limit of diffusion-controlled rate constants at the maximum coverage is equal to $k_{\text{LH}}^{\text{d}} \approx 4D_{\text{s}}$.²⁰ In our modeling, we accept that the surface-diffusion coefficient of the OH radicals is close to the diffusion coefficient of the H_2O molecules in the gas–solid and gas–liquid interface, $D_{\text{s}} \approx 10^{-5} \text{ cm}^2/\text{s}$.^{27–30} In this case, $k_{\text{LH}}^{\text{d}} \approx 4 \times 10^{-5} \text{ cm}^2/\text{s} \ll k_{\delta}$. Thus, we can assume that the LH surface recombination of the OH radicals is controlled by the surface diffusion, $k_{\text{LH}} \approx k_{\text{LH}}^{\text{d}}$. Moreover, according to eq 12, the diffusion rate constant drops with decreasing surface coverage; therefore, two-dimensional kinetics is limited by diffusion for the OH recombination.

Role of Defects. It is well-known that the surface heterogeneity is a critical parameter in the surface-reaction kinetics.^{13,25} The application of Langmuir adsorption is based on the suggestion that the surface is homogeneous and that the heat of adsorption Q has the same value for all active sites. On a realistic heterogeneous catalytic surface, the heat of adsorption may vary substantially in a large range from Q_{min} to Q_{max} . The analytical description of the surface heterogeneity is very complicated and requires various mathematical approaches. In particular, the role of quenched impurities on the surface kinetics for a large adsorbate coverage ($\theta > 0.1$) was studied by several groups.^{31,32} In our modeling, we used the simplification that the catalytic surface has active sites with the same values for the heat of adsorption. The adsorption of the radicals occurs on specific sites, such as defect structures on the surface of the crystal.¹³ In this case, the rate of adsorption is proportional to the free sites, $\theta_{\text{d}} - \theta$, where θ_{d} and θ are the coverages of defects and adsorbed radicals, respectively.

The surface density of Na^+Cl^- ionic pairs is 6.4×10^{14} molecules/ cm^2 , and the average fraction of the defects can reach 0.2.^{33,34} As pointed out by Kelly et al.,³⁵ the ionic crystal, such as NaCl, contains both dislocation and point defects. At equilibrium, the numbers of anion and cation defects are very nearly equal. Moreover, the presence of an impurity can cause the formation of the point defects in the ionic crystal. As shown above, the defect configuration on the surface was not considered in the continuum model (eq 12).

To understand the role of randomly distributed point defects on the diffusion-controlled reaction, we performed a MC simulation, developed by Allen and Seebauer.²⁰ Note that the result of the MC simulation for the case of the steady-state configuration gives useful information about coverage-dependent values of the steady-state rate constant. The MC measurements of diffusion-controlled rate constants were monitored using the dependence of the normalized rate constant, $k_{\text{LH}}^{\text{d}}/4D$, on the instantaneous total coverage, θ . The monitoring of neighbor concentrations and instant total concentration of radicals, θ_0 , was performed to predict the diffusion-controlled rate constant

from a modified Fick's law (for square-lattice geometry):²⁰

$$k_{\text{LH}}^{\text{d}} = 4D \frac{\theta_{\text{nm}}}{\theta_{\infty}} \quad (14)$$

where θ_{nm} is the coverage of nearest neighbors and θ_{∞} is the uniform-field coverage, which is determined by the concentration of radicals observed at large distance between the two nearest species.

The simulation of the recombination of radicals was carried out for a square lattice patch of the size 2000×2000 . The periodic boundary conditions were applied to extend the lattice patch. Randomly distributed radicals can migrate in random directions on defect sites. The reaction of annihilation occurred with unit probability if the OH radical migrated on occupied sites. Initially, the diffusion rate constant was calculated with the defect coverage $\theta_{\text{d}} = 1$. In the second stage, the concentration of randomly distributed defects θ_{d} was decreased. In this case, radicals can migrate on defect sites only. Temporal behavior of the normalized rate constant $k_{\text{LH}}^{\text{d}}/4D$ for initial radical coverage $\theta_0 = 9.1 \times 10^{-2}$ is presented in Figure 1a. For defect coverage $\theta_{\text{d}} = 1$, the normalized rate constant reached the steady-state configuration during the first few hops of an average coverage. The initial fast drop of the k_{LH}^{d} (first few hops) is related with statistical reorganization of the radicals for the short-lived transient regime.²⁰ The coverage-dependent values of the steady-state rate constant for the continuum model (eq 12) and MC calculations (eq 14) are presented in Figure 1b by curves 1 and 2, respectively. As shown in Figure 1b, the steady-state rate constant decreased from the collision limitation $4D$ and asymptotically reached the diffusion-limited rate constant for the continuum model (eq 12) at low coverage of the radicals.

The results of the MC simulation for the case of $\theta_{\text{d}} = 0.2$ are also presented in Figure 1a. As expected, at high initial concentration of radicals, the normalized rate constant dramatically dropped with a decrease in the concentration of the radicals. Note that, at high initial radical coverage, the rate of annihilation in the case of the defect coverage did not reach steady-state equilibrium. This effect is explained by the fact that a considerable part of the radicals remained on isolated defects and did not annihilate.

In the case of low initial coverage of radicals, the behavior of radical migration on the defect surface is close to the migration on the surface without heterogeneities. Figure 2 shows the result of MC simulation at low initial coverage of radicals, $\theta_0 = 3.80 \times 10^{-3}$. Radicals migrated on the defect structure with random defect distribution, $\theta_{\text{d}} = 0.2$. (The initial surface concentration of radicals $\theta_0 = 3.80 \times 10^{-3}$ corresponded to the Langmuir coverage at the free energy of the adsorption $E_{\text{ads}} \sim 15$ kcal/mol; for a real system, such as OH + NaCl, the coverage did not exceed 10^{-6} , see below.) When the kinetic process reached its quasi-equilibrium (average time was higher than four to five hops), the diffusion-limited rate constant had a steady-state solution and asymptotically was close to the solution (eq 12). Thus, we can assume that the diffusion-limited rate constant does not depend on the random defect configuration if the initial radical surface concentration is negligibly smaller than the defect concentration. Therefore, we can apply eq 12 with good accuracy to estimate the surface-diffusion-limited rate constant.

Results and Discussion

Modeling of the OH Uptake Process. The kinetics of the change of the surface coverage of OH radicals can be de-

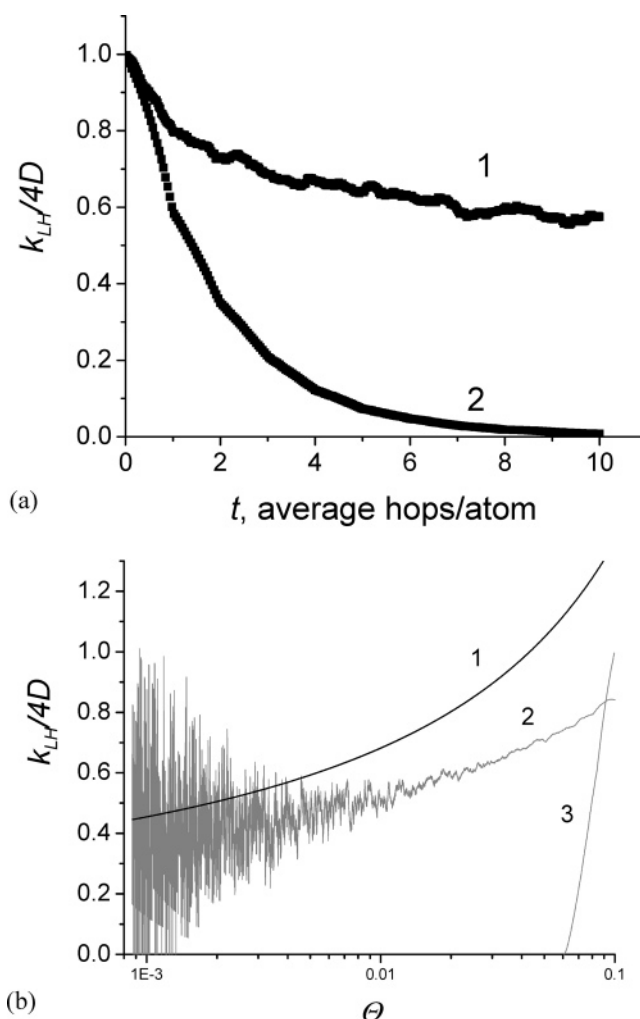


Figure 1. (a) Temporal behavior of the normalized rate constant, $k_{\text{LH}}^{\text{d}}/4D$, at the initial coverage of radicals, $\theta = 9.1 \times 10^{-2}$. MC simulation of the diffusion-limited rate constant was carried out for different defect coverages: $\theta_{\text{d}} = 1$ (1) and 0.2 (2). The rate constant reached the steady-state configuration at $\theta_{\text{d}} = 1$ (1). (b) The dependence of the normalized rate constant, $k_{\text{LH}}^{\text{d}}/4D$, on OH coverage, θ , for the continuum model (1), and MC calculations at $\theta_{\text{d}} = 1$ (2) and $\theta_{\text{d}} = 0.2$ (3), respectively. Initial coverage of radicals was 0.15. The rate constant decreased from the collision limitation $4D$ and asymptotically reached the diffusion-limited rate constant for the continuum model (eq 12) at low coverage of the radicals. The curve (3) demonstrates that, at high initial concentration of radicals, the normalized rate constant dramatically dropped with the decreasing of the concentration of radicals.

scribed by reactions 4 and 6, taking into account the defect coverage θ_{d} :

$$SZ \frac{d\theta_{\text{OH}}}{dt} = [k_1 n_{\text{OH}}(\theta_{\text{d}} - \theta_{\text{OH}}) - k_{-1} \theta_{\text{OH}} Z - k_{\text{ER}} n_{\text{OH}} \theta_{\text{OH}} Z - 2k_{\text{LH}} \theta_{\text{OH}}^2 Z^2] S \quad (15)$$

where n_{OH} (in cm^{-3}) is the gas-phase concentration of OH radicals, S is the area of the solid surface, and θ_{d} is the defect coverage. The θ_{d} value was set equal to the average fraction of the NaCl sites occupied by the defects at the NaCl surface, that is, $\theta_{\text{d}} = 0.2$.³⁴ For the adsorption rate constant k_1 , it can be assumed that gas-phase molecules striking the liquid-phase surface will thermally accommodate with a probability close to one, in this case $k_1 = c_{\text{OH}}/4$.

As shown above, the rate constants k_{ER} and k_{LH} are determined by eqs 10 and 12, respectively. The rates of interaction

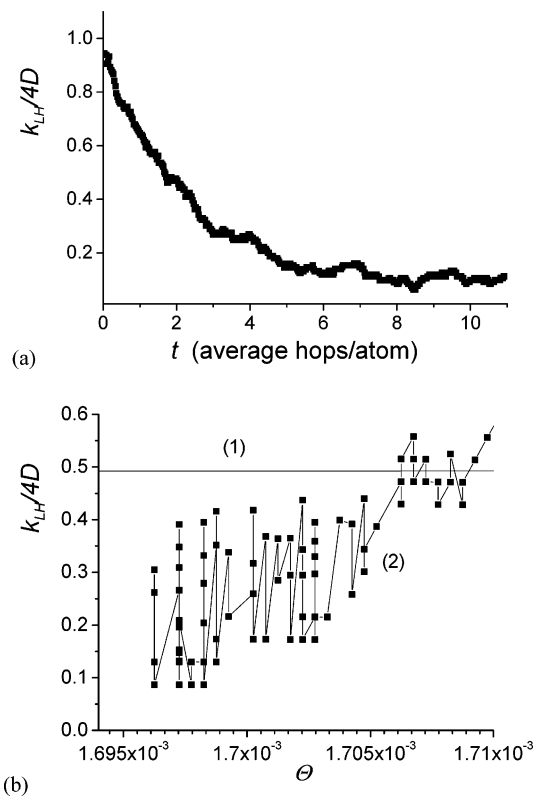


Figure 2. (a) Temporal behavior of the normalized rate constant, $k_{LH}/4D$, at low initial coverage of radicals, $\theta_0 = 3.80 \times 10^{-3}$. Radicals migrated on the defect structure with random point defect distribution, $\theta_d = 0.2$. The initial surface concentration of radicals ($\theta_0 = 3.80 \times 10^{-3}$) was much smaller than the defect concentration, $\theta_0 \ll \theta_d$. The rate constant reached the steady-state configuration. (b) The dependence of the normalized rate constant, $k_{LH}/4D$, on OH coverage for the continuum model (1) and MC calculations (2; $\theta_0 = 3.80 \times 10^{-3}$, $\theta_d = 0.2$).

of the gas-phase species, OH, with the solid surface are described by the following expressions:

$$V \frac{dn_{OH}}{dt} = [-k_1 n_{OH}(\theta_d - \theta_{OH}) + k_{-1} \theta_{OH} Z - k_{ER} n_{OH} \theta_{OH} Z] S \quad (16)$$

where V is the volume. The uptake coefficient γ is experimentally determined from eq 17:

$$V \frac{dn_{OH}}{dt} = -\frac{\gamma_{OH} c_{OH}}{4} n_{OH} S \quad (17)$$

The characteristic time of the establishment of the steady-state radical uptake is determined by the fast adsorption process. In this case, the characteristic time of establishing the steady-state radical uptake is shorter than the duration of the experiment, $\tau \sim 4S/c_{OH}V$ (S/V is the ratio of the surface to the volume of the reactor). When the quasi-equilibrium conditions ($dn_{OH}/dt = 0$) are taken into account, transformations of eqs 15–17 give a simple relation between the surface coverage of the radicals and the measured uptake coefficient:

$$\gamma = (2k_{ER} n_{OH} \theta_{OH} Z + 2k_{LH} \theta_{OH}^2 Z_{OH}) / (k_1 n_{OH}) \quad (18)$$

$$k_{-1} = \frac{k_1 n_{OH}(\theta_d - \theta_{OH}) - \frac{\gamma_{OH} c_{OH}}{4} + k_{ER} n_{OH} \theta_{OH} Z_{OH}}{\theta_A Z} \quad (19)$$

TABLE 2: Kinetic Parameters for the Modeling of the OH Uptake by the Solid Surface for Schemes 4–6

T	295 K
surface diffusion, $D_s^{27-30,41}$	$10^{-5} \text{ cm}^2/\text{s}$
k_{ER}	eq 10
k_{LH}	eq 12
defect coverage, θ_d^{34}	0.2
concentration of OH radicals	$2 \times 10^6 - 5 \times 10^{10} \text{ cm}^{-3}$

In eq 18, the first and second terms describe ER and LH mechanisms, respectively. The parameters of the modeling are summarized in Table 2. The universal dependence of the uptake coefficient on the adsorbed radicals in eq 18 is presented in Figure 3. The modeling was carried out at two OH concentrations ($2 \times 10^6 \text{ radicals/cm}^3$ and $5 \times 10^{10} \text{ radicals/cm}^3$). As shown in Figure 3, at the concentration of OH radicals close to actual atmospheric conditions ($2 \times 10^6 \text{ radicals/cm}^3$), the LH mechanism is more effective in comparison with the ER scheme.

Because the LH reaction scheme is more effective than the ER scheme (it means that the first term is much smaller than the second term in eq 18), the uptake coefficient has a strong dependence on the OH concentration in the gas phase. For example, at $E_{OH} = 10 \text{ kcal/mol}$, the OH uptake coefficient dramatically drops from 10^{-3} to 10^{-7} in the case of decreasing OH concentration in the gas phase from 5×10^{10} to $5 \times 10^6 \text{ cm}^{-3}$, respectively. The dependence of the uptake coefficient on the OH concentration is shown in Figure 4. The result of this modeling clearly demonstrates that the laboratory experimental data should be extrapolated to actual atmospheric conditions in a proper way to find the real effect of heterogeneous reactions on the OH balance in the troposphere.

The adsorption energy was found from the experimental values of the uptake coefficients by solving the transcendent eqs 18 and 19. For this purpose, the adsorption energy was fitted from the curve $E_{OH}(\theta_{OH})$ giving the best match to the coverage dependence of the uptake coefficient. From eq 19, the coverage dependence of the adsorption energy is shown in Figure 5. Experimental data of OH uptake by dry salt surfaces (NH_4HSO_4 , $(\text{NH}_4)_2\text{SO}_4$,³ NaCl ,⁴ NH_4NO_3 ,⁴ and Al_2O_3 ,³⁶) are summarized on the theoretical curve of the uptake coefficient in Figure 5. The filled circles in Figure 5 show the adsorption energy

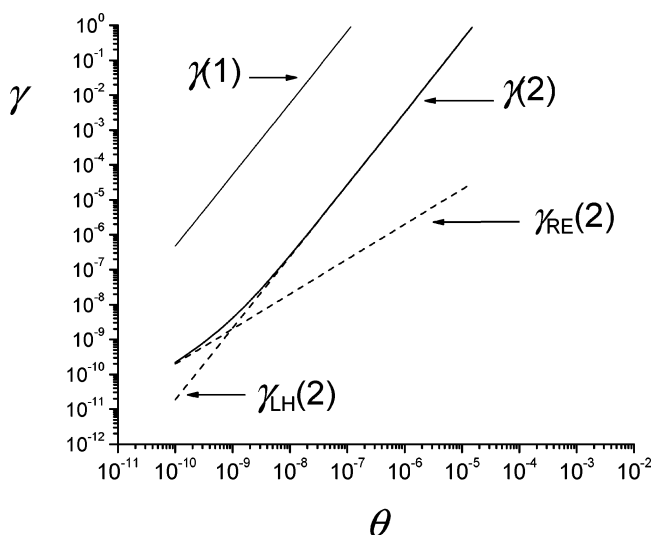


Figure 3. The dependence of the OH uptake coefficient on OH coverage. The reaction of the recombination of OH radicals on the surface is limited by the surface diffusion. The figure shows two coverage dependencies at a typical atmospheric OH concentration of 10^6 cm^{-3} (1) and at experimental conditions of OH concentrations of $5 \times 10^{10} \text{ cm}^{-3}$ (2), respectively.

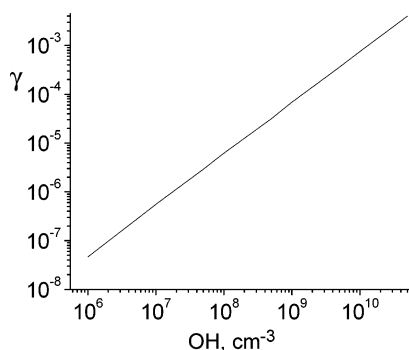


Figure 4. Concentration dependence of the uptake coefficient. The modeling was calculated from eqs 18 and 19 using Table 2 and $E_{OH} = 10$ kcal/mol.

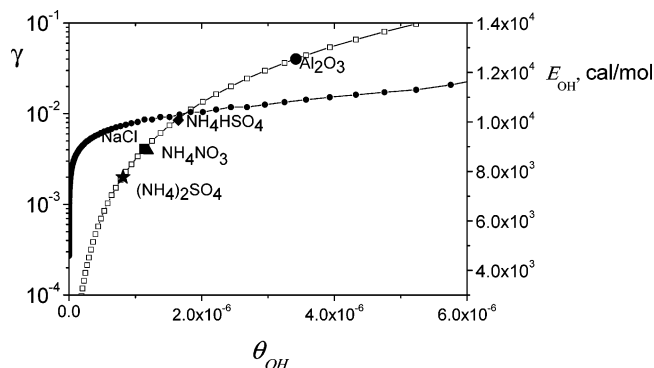


Figure 5. Uptake $\gamma(\theta_A)$ (\square) and adsorption energy E_{OH} (\bullet) dependencies on coverage from eqs 18 and 19. The measured uptake coefficient for the NH_4HSO_4 ,³ $(NH_4)_2SO_4$,³ NaCl,⁴ NH_4NO_3 ,⁴ and Al_2O_3 ³⁶ are summarized on the curve $\gamma(\theta_A)$.

TABLE 3: Calculated Adsorption Free Energies

substrate	uptake coefficient	T , K	E_{OH} , kcal/mol
$(NH_4)_2SO_4$	0.0085 ³	296	10.3
NH_4HSO_4	0.002 ³	296	9.8
NaCl	4.1×10^{-3} ⁴	300	10.2
NH_4NO_3	3.9×10^{-3}	300	10.2
Al_2O_3	0.04 ³⁶	295	11.0
	0.11 ⁴⁰	295	11.7
water ice	0.03 ± 0.02 ³	205–230	7.3–7.6

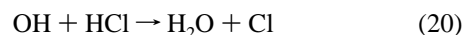
dependence on the coverage. The calculated $E_{OH}(\theta_{OH})$ is presented in Table 3. As shown in Figure 5 and Table 3, the adsorption energy for salt Al_2O_3 is in the range 9.8–11 kcal/mol. For solid salts, the adsorption energy does not exceed 10.2 kcal/mol. This value is very close to the adsorption energies for the physisorption of water on NaCl (100).³⁷

Atmospheric Implications

According to the presented model (see Figure 4), the predicted uptake coefficient is in the range $\sim 10^{-7}$ – 10^{-6} at an atmospheric concentration of the OH radicals of $\sim 10^6$ radicals/cm³. Thus, the direct heterogeneous decay of OH radicals on solid aerosols does not change the total balance of OH radicals in the troposphere as a result of the high reactivity of OH radicals in the gas phase.

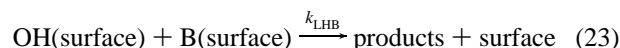
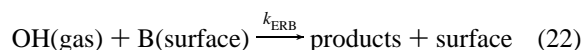
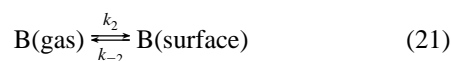
However, the solid aerosols can promote the corresponding chemical reaction of OH radicals with adsorbed pollutants, such as VOCs, inorganic molecules, and semi-volatile organic compounds (SVOCs). There are several experimental studies where the catalytic promotion by solid aerosols was studied for the reaction of OH radicals with adsorbed molecules. The increase of the OH uptake by salt in the presence of 1-hexanol

was observed by Cooper and Abbatt.³ The role of VOCs on the heterogeneous chemistry of OH radicals in the presence of solid surfaces of atmospheric interest was studied by Oh and Andino and by Sorensen and co-workers.^{3,9–12} As mentioned in the introduction, Sorensen et al. and Oh and Andino obtained different results in the study of the heterogeneous reactions of OH radicals with volatile compounds such as CH_3OH , C_2H_5OH , and $n-C_3H_7OH$. The explanation for this contradiction was presented by Sorensen et al. on the basis of the ER scheme of the reaction of OH with adsorbed VOC. They proved that the reactions of OH radicals with weakly adsorbed organics cannot influence the total decay of OH radicals in the gas phase. The heterogeneous reaction of OH radicals with CO adsorbed on a solid NaCl surface was studied by Hack et al.³⁸ They found that the rate of depletion of OH radicals was significantly increased in the reactor when the CO gas was added. Cooper and Abbatt³ demonstrated that the OH uptake on ice could be considerably increased by either adsorbing HNO_3 to the surface or melting the ice surface by exposure to HCl. Note that the reaction between OH and HCl with direct formation of atomic chlorine is fast in the gas phase (where the conditions for reaction are k (cm³ molecule^{−1} s^{−1}) = $4.2 \times 10^{-13}(T/298 \text{ K})^{1.66}e^{0.37(\text{kcal/mol})/RT}$ and $k = 7.84 \times 10^{-13}$ cm³ molecule^{−1} s^{−1} at 300 K).³⁹



In the case of the adsorption of HCl on the solid surfaces, such as ice or salts, the reaction of hydroxyl radicals with hydrochloric acid can occur via the LH mechanism¹³ leading to the formation of reactive chlorine on the solid surface. It is not clear under what conditions the heterogeneous loss rate of OH radicals can exceed the corresponding homogeneous gas-phase reaction rate.

As shown above, the uptake coefficient for the schemes 4–6 has a strong dependence on the OH concentration both in the gas phase and on the surface. Let us consider a hypothetical adsorbed reagent, B, for which a significant fraction of adsorbed molecules can interact with OH radicals through the following heterogeneous reactions 21–23. The possible reagent B may be a SVOC, such as di(2-ethylhexyl)phthalate (vapor pressure, 1.8×10^{-7} Torr at 298 K):



where k_2 and k_{-2} are the adsorption and desorption rate constants for molecule B and k_{ERB} and k_{LHB} are the ER and LH reaction rate constants according to schemes 22 and 23, respectively.

The coverage of adsorbed OH radicals and B molecules is determined by the following equations:

$$0 = k_1 n_{OH}(\theta_d - \theta_{OH} - \theta_B) - k_{-1} \theta_{OH} Z - k_{LHB} \theta_{OH} \theta_B Z^2 - 2k_{LH} \theta_{OH} \theta_{OH} Z^2 \quad (24)$$

$$0 = k_2 n_B(\theta_d - \theta_{OH} - \theta_B) - k_{-2} \theta_B Z - k_{ERB} n_{OH} \theta_B Z - k_{LHB} \theta_{OH} \theta_B Z^2 \quad (25)$$

TABLE 4: Kinetic Parameters for the Modeling of the OH Uptake in the Case of the Reaction of OH Radicals with Adsorbed Molecules B According to Schemes 21–23

T	295 K
surface diffusion, $D_s^{27-30,41}$	10^{-5} cm ² /s
k_{ERB}	eq 10
k_{LH}	eq 12
defect coverage, θ_d^{34}	0.2
concentration of OH radicals	2×10^6 cm ⁻³
concentration of B molecules	5×10^9 cm ⁻³
E_{OH} (this work)	10 kcal/mol
adsorption energy, E_B	9–16 kcal/mol
concentration of the aerosols, N_a	1000 cm ⁻³
radius of aerosols	1 μ m

The expression for the probability of the OH uptake γ_{OH} has the form

$$\gamma_{\text{OH}} = \frac{1}{k_1 n_{\text{OH}}} [k_1 n_{\text{OH}} (\theta_d - \theta_{\text{OH}} - \theta_B) - k_{-1} \theta_{\text{OH}} Z + k_{\text{ERB}} n_{\text{OH}} \theta_B Z] \quad (26)$$

Note that we used the result of our modeling that the ER scheme cannot give a considerable contribution to the OH uptake (eq 5). Therefore, we excluded the term $k_{\text{ERB}} n_{\text{OH}} \theta_B Z$ in the modeling. For simplicity, we assumed that k_{ERB} and k_{LHB} are expressed by eqs 10 and 12, respectively (it gives the lower limit to the uptake process for the schemes 21–23).

It is very interesting to compare the gas-phase reaction and heterogeneous reaction $\text{OH} + \text{B}$. The heterogeneous reaction rate W_{het} of the reaction $\text{OH} + \text{B}$ is determined by the following equation (for nondiffusion kinetics in the gas phase):

$$W_{\text{het}} = 4\pi r_a^2 \frac{\gamma_{\text{C}}}{4} N_a \quad (27)$$

where πr_a^2 is a surface area of the aerosol of the size r_a and N_a is the concentration of the particles. Kinetic parameters for the modeling are summarized in Table 4. We used the parameters for aerosols (N_a , r_a) for a typical urban air mass. The energy of adsorption for OH radicals was taken for solid NaCl, that is, ~ 10 kcal/mol, see Table 3.

The modeling showed that the contribution of the ER reaction scheme (third term in eq 26) at $E_B = 9$ kcal/mol did not exceed 1% to the total uptake process. The influence of the ER reaction became more considerable at high values of E_B ; for example, the contribution of the ER reaction was $\sim 10\%$ at $E_B = 15$ kcal/mol. The result of the modeling of the heterogeneous reaction rate for the schemes 21–23 is presented in Figure 6. As shown in Figure 6, the heterogeneous reaction rate for the reaction of

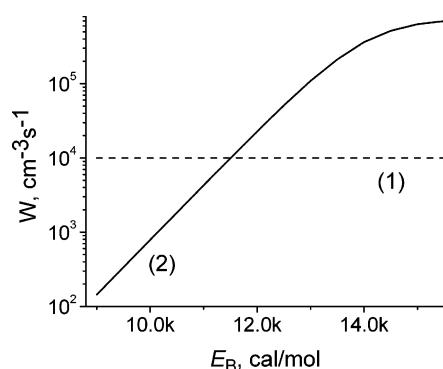


Figure 6. Comparison of the gas-phase reaction rate $\text{OH} + \text{B}$ ($k = 10^{-12}$ cm³/s; 1) with the heterogeneous reaction rate (2) for the reaction of OH radicals with molecules B adsorbed on nonreactive aerosols. E_B is the adsorption energy of molecules B.

OH with adsorbed reagent B can exceed the corresponding gas-phase reaction $\text{OH} + \text{B}$ when B is a strongly adsorbed molecule, such as a SVOC. Obviously, the heterogeneous reaction of OH radicals with the weakly adsorbed molecules, for example, HCl, VOC, and CO, cannot compete with the corresponding gas-phase reaction. Thus, the result of this modeling partially confirms the experimental results of Sorensen et al.:¹² solid aerosols coated with weakly adsorbed organics, such as VOCs, cannot promote the heterogeneous reaction of OH radicals.

Conclusion

We carried out a simulation of the uptake process of OH radicals for a nonreactive solid substrate. On the basis of the suggestion of a diffusion-limited recombination reaction on the surface, we estimated the adsorption free energy for the solids of atmospheric interest. The analysis of the OH uptake process indicates that the kinetics of heterogeneous chemical reactions involving the OH radical under atmospheric conditions can be interpreted in the frame of the LH model without taking into account the surface heterogeneities. The calculated values of the adsorption energies can be used to simulate the heterogeneous processes of OH radicals with adsorbed reagents, such as SVOCs. An appropriate approach to the description of the uptake should involve the combination of both ER and LH schemes.

References and Notes

- (1) Djikaev, Y. S.; Tabazadeh, A. *J. Geophys. Res., [Atmos.]* **2003**, *108*, 4689.
- (2) Atkinson, R.; Arey, J. *Atmos. Environ.* **2003**, *37*, S197–S219.
- (3) Cooper, P. L.; Abbatt, J. P. D. *J. Phys. Chem.* **1996**, *100*, 2249–2254.
- (4) Ivanov, A. V.; Gershenzon, Y. M.; Gratpanche, F.; Devolder, P.; Sawersyn, J. P. *Ann. Geophys.* **1996**, *14*, 659–664.
- (5) Msibi, I. M.; Li, Y.; Shi, J. P.; Harrison, R. M. *J. Atmos. Chem.* **1994**, *18*, 291–300.
- (6) Timonen, R. S.; Chu, L. T.; Leu, M. T.; Keyser, L. F. *J. Phys. Chem.* **1994**, *98*, 9509–9517.
- (7) Rudich, Y.; Talukdar, R. K.; Ravishankara, A. R. *J. Geophys. Res., [Atmos.]* **1996**, *101*, 21023–21031.
- (8) Vogt, R.; Finlayson-Pitts, B. J. *J. Phys. Chem.* **1994**, *98*, 3747–3755.
- (9) Oh, S.; Andino, J. M. *Atmos. Environ.* **2000**, *34*, 2901–2908.
- (10) Oh, S.; Andino, J. M. *Int. J. Chem. Kinet.* **2001**, *33*, 422–430.
- (11) Oh, S.; Andino, J. M. *Atmos. Environ.* **2002**, *36*, 149–156.
- (12) Sorensen, M.; Hurley, M. D.; Wallington, T. J.; Dibble, T. S.; Nielsen, O. J. *Atmos. Environ.* **2002**, *36*, 5947–5952.
- (13) Adamson, A. W. *The physical chemistry of surfaces*; Wiley & Sons: New York, 1990.
- (14) Clark, A. *The Theory of Adsorption and Catalysis*; Academic Press: New York and London, 1970.
- (15) Ammann, M.; Poschl, U.; Rudich, Y. *Phys. Chem. Chem. Phys.* **2003**, *5*, 351–356.
- (16) Remorov, R. G.; Gershenzon, Y. M.; Molina, L. T.; Molina, M. J. *J. Phys. Chem. A* **2002**, *106*, 4558–4565.
- (17) Sander, S. P.; Friedl, R. R.; Ravishankara, A. R.; Golden, D. M.; Kolb, C. E.; Kurylo, M. J.; Huie, R. E.; Orkin, V. L.; Molina, M. J.; Moortgat, G. K.; Finlayson-Pitts, B. J. *Chemical Kinetics and Photochemical Data for Use in Atmospheric Studies*; Evaluation Number 14, JPL Publication 02-25, NASA, Jet Propulsion Laboratory; California Institute of Technology: Pasadena, CA, 2003.
- (18) Clark, A. *The Theory of Adsorption and Catalysis*; Academic Press: New York and London, 1970.
- (19) Freeman, D. L.; Doll, J. D. *J. Chem. Phys.* **1983**, *78*, 6002–6009.
- (20) Allen, C. E.; Seebauer, E. G. *J. Chem. Phys.* **1996**, *104*, 2557–2565.
- (21) Montroll, E. W. *J. Math. Phys.* **1969**, *10*, 753–765.
- (22) Berezhkovskii, A. M.; Zitserman, V. Y.; Polimeno, A. *J. Chem. Phys.* **1996**, *105*, 6342–6357.
- (23) Khairutdinov, R. F.; Burshtein, K. Y.; Serpone, N. *J. Photochem. Photobiol., A* **1996**, *98*, 1–14.
- (24) Deminsky, M.; Knizhnik, A.; Belov, I.; Umanskii, S.; Rykova, E.; Bagatur'yants, A.; Potapkin, B.; Stoker, M.; Korkin, A. *Surf. Sci.* **2004**, *549*, 67–86.

- (25) Tovbin, Y. K. *Prog. Surf. Sci.* **1990**, *34*, 1–235.
- (26) Kammeyer, C. W.; Whitman, D. R. *J. Chem. Phys.* **1972**, *56*, 4419–4421.
- (27) Paul, S.; Chandra, A. *Chem. Phys. Lett.* **2003**, *373*, 87–93.
- (28) Sakuma, H.; Tsuchiya, T.; Kawamura, K.; Otsuki, K. *Mol. Simul.* **2004**, *30*, 861–871.
- (29) Liu, P.; Harder, E.; Berne, B. J. *J. Phys. Chem. B* **2004**, *108*, 6595–6602.
- (30) Shinto, H.; Sakakibara, T.; Higashitani, K. *J. Phys. Chem. B* **1998**, *102*, 1974–1981.
- (31) Nikunen, P.; Vattulainen, I.; Ala-Nissila, T. *J. Chem. Phys.* **2002**, *117*, 6757–6765.
- (32) Zhdanov, V. P.; Kasemo, B. *J. Chem. Phys.* **1998**, *108*, 4582–4590.
- (33) Kittel, C. *Introduction to Solid State Physics*; Wiley & Sons: New York, 1986.
- (34) Dai, D. J.; Ewing, G. E. *J. Chem. Phys.* **1993**, *98*, 5050–5058.
- (35) Kelly, A.; Groves, G. W.; Kidd, P. *Crystallography and Crystal Defects*, Revised Edition; Wiley & Sons: Toronto, 2000.
- (36) Gershenzon, Y. M.; Ivanov, A. V.; Kucheryavii, S. I.; Lyapunov, A. Y.; Rozenshtein, V. B. *Kinet. Catal.* **1986**, *27*, 928–932.
- (37) Meyer, H.; Entel, P.; Hafner, J. *Surf. Sci.* **2001**, *488*, 177–192.
- (38) Hack, W.; Vardanyan, L.; Wagner, H. G. *Ber. – Max-Planck-Inst. Stromungsforsch.* **1997**, *13*, 1–19.
- (39) Battin-Leclerc, F.; Kim, I. K.; Talukdar, R. K.; Portmann, R. W.; Ravishankara, A. R. *J. Phys. Chem. A* **1999**, *103*, 3237–3244.
- (40) Bertram, A. K.; Ivanov, A. V.; Hunter, M.; Molina, L. T.; Molina, M. J. *J. Phys. Chem. A* **2001**, *105*, 9415–9421.
- (41) Do, D. D. *Adsorption Analysis: Equilibria and Kinetics*; Imperial College Press: London, 1998.